



Practical study on the impact of injection conditions in gradient elution mode for the analysis of therapeutic proteins when using very short columns

Raquel Pérez-Robles^{a,b,c}, Szabolcs Fekete^d, Natalia Navas^{a,b}, Davy Guillarme^{e,f,*}

^a Instituto de Investigación Biosanitaria de Granada (ibs.GRANADA), Granada, Spain

^b Department of Analytical Chemistry, Science Faculty, University of Granada, Granada, Spain

^c Fundación para la Investigación Biosanitaria de Andalucía Oriental-Alejandro Otero, Granada, Spain

^d Waters Corporation, Geneva, Switzerland

^e School of Pharmaceutical Sciences, University of Geneva, CMU - Rue Michel Servet 1, 1211 Geneva 4, Switzerland

^f Institute of Pharmaceutical Sciences of Western Switzerland, University of Geneva, CMU - Rue Michel Servet 1, 1211 Geneva 4, Switzerland

ARTICLE INFO

Keywords:

Loading capacity
injection volume
ultra-short columns
monoclonal antibodies
proteins
ion exchange chromatography

ABSTRACT

The impact of injected sample volume on apparent efficiency has been studied for very short columns in a systematic way. For large molecules such as therapeutic proteins, it was found that relatively large volumes can be injected onto ultra-short RPLC and IEX columns (i.e. $L < 50$ mm) without significantly affecting the quality of the separation. This favourable behavior is due to the on-off elution mechanism of large molecules and to the fact that therapeutic protein samples are formulated in aqueous-based media, which is the weakest solvent in RPLC and IEX. Therefore, their peak is strongly focused at the column inlet even when large volume is injected, and pre-column peak dispersion is compensated. However, ultra-short HILIC columns do not seem to be favorable, as they require for very low injection volume to avoid detrimental peak splitting and breakthrough effects. Such peak distortion is related to the inherent solvent mismatch between sample diluent (aqueous) and mobile phase strength (highly organic in HILIC). When studying mass load, the ranking of the elution modes was the same, and the largest relative mass could be injected onto IEX columns (as large as 10% sample to sorbent mass), without affecting the separation quality.

1. Introduction

Chromatography has taken a prominent place in the characterization and analysis of proteins today [1]. Although reversed-phase chromatography (RPLC) is the foremost chromatography technique used for this purpose, other techniques such as ion-exchange (IEX), size-exclusion (SEC), hydrophilic-interaction (HILIC), and hydrophobic-interaction (HIC) chromatography play very specific roles in characterizing and analyzing protein drugs. Each of the above-mentioned chromatographic modes has the capability to provide different and complementary information for the complete characterization of proteins.

In general, large solutes - such as proteins -, have a particular elution behavior in chromatography. They are extremely sensitive to mobile phase composition, and a very small change in eluent strength can result in complete release of the molecule from the column. This behavior is

often referred as "on-off" mechanism, which involves only a small number of adsorption-desorption steps rather than a multiple-step partitioning process, which is typical for small molecules. This particular mechanism involves two considerations on the column length (L) and gradient profile [2]. Several studies have concluded that column length has little effect on their separation, and short or ultra-short columns (5 or 10 mm long) are clearly advantageous for protein separations, as operating pressure and analysis time can be reduced, while maintaining resolution [3–6].

Ultra-high pressure liquid chromatography (UHPLC) instrumentation plays an equally important role in achieving excellent chromatographic performance as the column itself. Instruments not only have to be capable of delivering the desired flow rate against the resistance exerted by the column, but also to add as little dispersion as possible to the analyte bands [7]. For ultra-short column separations, an optimized

* Corresponding author at: Davy Guillarme, Institute of Pharmaceutical Sciences of Western Switzerland (ISPSO), School of Pharmaceutical Sciences, University of Geneva, CMU - Rue Michel Servet 1, 1211 Geneva 4, Switzerland.

E-mail address: davy.guillarme@unige.ch (D. Guillarme).

<https://doi.org/10.1016/j.chroma.2023.464359>

Received 25 July 2023; Received in revised form 31 August 2023; Accepted 1 September 2023

Available online 10 September 2023

0021-9673/© 2023 The Author(s). Published by Elsevier B.V. This is an open access article under the CC BY license (<http://creativecommons.org/licenses/by/4.0/>).

low-dispersion instrument is mandatory to take the full benefits of very small volume columns. Therefore, the instrument should be able to manage low dwell volume, very small extra column variance, short injection cycle time, small enough injection volume and appropriate data acquisition rate.

Extra-column volume effects, caused by dispersion in different parts of the chromatographic system outside the column bed (including extra-bed contributions too), influence the shape of peaks eluted from the column and their apparent retention, especially for ultra-short columns (with very low column volumes) [8]. The extra-column peak dispersion, is a function of the flow rate, sample diffusion coefficient, mobile phase viscosity, temperature, and injected volume [9,10]. In ultra-short column separations, the column volume and associated volume band variance is inherently low due to the limited column volume, and is therefore highly affected by the extra-column band variance. With this in mind, it is needed to use very well controlled conditions, in which the extra-column contributions are kept to a minimum.

Another factor to take into account is the sample amount injected into the column in terms of both extra-column band broadening and overload effects (related to the loading capacity of the column) [11,12]. However, it worth mentioning that most of the pre-column dispersions are compensated in gradient elution mode, if the initial retention of the solute at the head of the column is high enough [13]. This so-called focusing effect is especially important for large solutes. Therefore, it is reasonable to assume that pre-column dispersion (including the dispersion occurring in the injector and in the pre-column tubing) is negligible for large molecule separations. Regarding sample injection, if there is no volumetric or mass overload, the peak height should change proportionally with the injected volume without affecting the width of the peak. However, if the injected sample volume is increased to a huge extent, at some point, the eluting peak will become broadened and distorted, due to overload effect [14]. Since the overload volume is proportional to column volume, it is therefore expected that the overload effect will occur at much smaller injected volumes for ultra-short columns than for larger ones ($L \geq 50$ mm), due to their very low column bed volume (V_{col}), (i.e. for a given flow rate and equal performance characteristics, the V_{col} decreases proportionally with the column length) [15].

Despite all the consideration discussed above, the short and ultra-short columns have already been applied successfully for proteins characterization using various chromatographic modes such as RPLC [3], IEX [4] and HILIC [5]. The use of very short columns has many advantages, i.e. providing acceptable performance compared to regular columns (100–150 mm length) in much shorter analysis time, they require much shorter equilibration time and the probability of on-column protein hydrolysis decreases significantly thanks to the shorter residence times. Sample consumption can also be decreased significantly, and ultra-short columns are also promising for multidimensional chromatographic separations.

In this work, the injection conditions have been systematically evaluated for very short column separations in RPLC, IEX and HILIC modes. To this end, the loading capacity of several ultra-short column prototypes (different column lengths, porosities and particle sizes) was compared with commercial longer columns, when analyzing therapeutic proteins and protein subunits having sizes comprised between 5 and 150 kDa.

2. Materials and Methods

2.1. Chemicals, reagents and sample preparation

Acetonitrile (ACN) and water were purchased from Fisher Scientific (Reinach, Switzerland). Trifluoroacetic acid (TFA), DL-dithiothreitol (DTT), potassium chloride (KCl), 2-(N-morpholino)ethanesulfonic acid (MES) monohydrate and MES sodium salt were purchased from Sigma-Aldrich (Buchs, Switzerland). Therapeutic proteins, i.e. MabThera™

(rituximab, 10 mg/mL) and Kineret™ (anakinra 150 mg/mL), were purchased from their respective manufacturers as EU pharmaceutical grade products. Insulin, USP specification quality grade was supplied by Sigma-Aldrich (Buchs, Switzerland).

Protein subunits such as the light (LC) and heavy (HC) chains were generated by reducing the rituximab disulphide bonds by the addition of 10 μ L DTT (1M) to 50 μ g of the monoclonal antibody (10 mg/mL), then the mixture was incubated for 30 min at 45°C. The final concentration was 5 mg/mL.

2.2. Chromatographic instrumentation

A Waters ACQUITY™ UPLC™ I-Class System equipped with a binary solvent delivery pump, autosampler (FTN), thermostatted column compartment, UV detector and fluorescence detector (FLR) was used for this study. Two detector flow-cells were used including a 2 μ L FLR and a 0.5 μ L UV cells. The extra-column volume was measured as $V_{EC} = 4.6$ μ L, while the gradient delay volume was $V_d = 100$ μ L. Data acquisition and instrument control were carried out using Empower™ Pro 3 Software (Waters).

2.3. Chromatographic conditions, columns

2.3.1. RPLC

The RP chromatographic separation was conducted using several commercial and prototype columns packed with different particles, i.e. fully porous (1.7 μ m and 2.5 μ m) and superficially porous (2.7 μ m) particles possessing various lengths ($L = 10, 50$ and 150 mm). All columns were provided by Waters (Milford, USA). A detailed column description is shown in Table 1. Intact rituximab (10 mg/mL), anakinra (150 mg/mL), rituximab LC (5 mg/mL) and rituximab HC (5 mg/mL) were diluted in pure water to obtain concentrations of 0.1, 0.25, 0.5, 0.75, 1, 2, 5 mg/mL.

The mobile phases used for RPLC separations were water + 0.1% TFA (mobile phase A) and ACN + 0.1% TFA (mobile phase B). Different injected volumes (0.1, 0.3, 0.5, 1, 2, 5 and 10 μ L) of several intact rituximab, anakinra and reduced rituximab subunits (HC and LC) sample concentrations (0.1 to 5 mg/mL) were injected. The samples were eluted with 30 to 45% B and the gradient time (t_G) was set at 0.8 min ($L = 10$ mm), 4.4 min ($L = 50$ mm) and 13 min ($L = 150$ mm) (t_G was adjusted proportionally with the column volume). The column temperature was set at 80 °C. The flow rate was set at 0.3 mL/min for all columns. Detection was carried out at $\lambda = 214$ and $\lambda = 280$ nm at sampling rate of 20 Hz and filter time constant of 0.05 s.

2.3.2. IEX

The IEX separations were carried out using commercial and prototype strong cation exchanger columns, provider by Waters. Three different columns were used (detailed in Table 1), i.e. SCX mAb 3 μ m in 2.1 \times 15 mm; 2.1 \times 20 mm and 2.1 \times 150 mm formats. Intact rituximab (10 mg/mL) and anakinra (150 mg/mL) were diluted in pure water to obtain 0.1, 0.3, 0.5, 0.75, 1, 2, 5 mg/mL sample solutions.

Salt gradient IEX separations were performed using 10 mM MES in water pH = 6 (mobile phase A) and 10 mM MES + 0.5 M KCl in water pH = 6 (mobile phase B). The MES buffer was prepared by mixing the acidic MES salt (MES monohydrate) with the basic MES sodium salt, until the final pH was reached. Different injected volumes (0.1, 0.3, 0.5, 1, 2, 5 and 10 μ L) of several intact rituximab and anakinra sample concentrations (0.1 to 5 mg/mL) were injected. A linear gradient from 30 to 50 % B was run, during 6, 8 and 20 min for the $L = 15, 20$ and 50 mm long columns, respectively. The flow rate was 0.2 mL/min. The column temperature was set at 25 °C and the FLD detection was recorded at $\lambda_{ex} = 280$ nm, $\lambda_{em} = 350$ nm with a sampling rate of 20 Hz and filter time constant of 0.05 s.

Table 1

Column specifications for RPLC, IEX and HILIC chromatographic modes.

	Column	Particle size (μm)	Internal diameter; i. d. (mm)	Column length; L (mm)	Column bed morphology	Stationary phase chemistry	Average pore diameter (\AA)
RPLC	Prototype	1.7	2.1	10	FPP; $\epsilon = 0.72$	C4	300
	Prototype	2.5	2.1	10	FPP; $\epsilon = 0.71$	C4	300
	Prototype	2.7	2.1	10	SPP; $\epsilon = 0.70$	polyphenyl	450
	ACQUITY UPLC Protein BEH C4, Waters.	1.7	2.1	50	FPP; $\epsilon = 0.69$	C4	300
	ACQUITY UPLC Protein BEH C4 300 \AA , Waters.	1.7	2.1	150	FPP; $\epsilon = 0.70$	C4	300
IEX	Prototype	3	2.1	15	NP; $\epsilon = 0.51$	SCX (sulphonic acid)	non-porous
	Prototype	3	2.1	20	NP; $\epsilon = 0.43$	SCX (sulphonic acid)	non-porous
	BioResolve SCX, Waters	3	2.1	50	NP; $\epsilon = 0.30$	SCX (sulphonic acid)	non-porous
HILIC	ACQUITY UPLC GlycoProtein BEH, amide, Waters.	1.7	2.1	50	FPP; $\epsilon = 0.74$	amide	300

2.3.3. HILIC

A Glycoprotein BEHTM Amide 300 \AA , 1.7 μm ; 2.1 \times 50 mm Commercial Column provided by Waters (Milford, USA) was used for the HILIC study (see specification in Table 1). The rituximab HC and LC (5 mg/ml), anakinra (150 mg/mL), and insulin (5 mg/mL) were diluted in three different mixtures of ACN/water; v/v (30/50; 50/50; and 50/50 + 0.1 % TFA respectively) to reach the required concentration.

The mobile phases were water + 0.1% TFA (mobile phase A) and ACN + 0.1% TFA (mobile phase B). Rituximab subunits (HC and LC), anakinra and insulin samples were injected in various volumes (0.1, 0.3,

0.5, 1, 2 μL) and concentrations (0.25 to 1 mg/mL). Linear gradients were applied from 72 to 64 % B for rituximab HC and LC, from 78 to 64% for anakinra and from 85 to 71 % of B for insulin over 10 min. The column temperature was set at 60 $^{\circ}\text{C}$ and the flow rate was 0.3 mL/min. The detection was carried out at $\lambda = 214$ and $\lambda = 280$ nm at sampling rate of 20 Hz and filter time constant of 0.005 s.

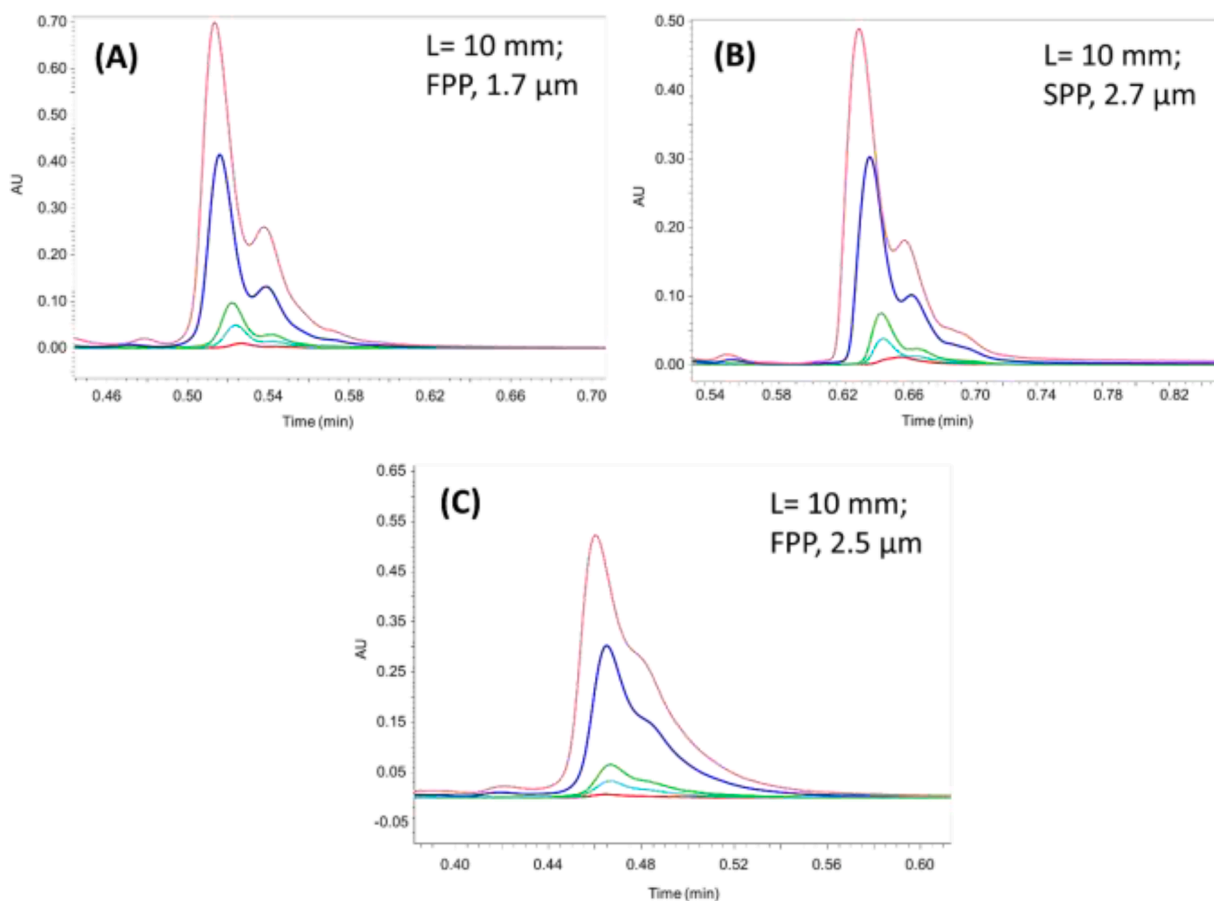


Fig. 1. Volumetric load in RPLC mode. Chromatograms of rituximab heavy chain (0.5 mg/mL) using several injected volumes, i.e. pink trace 10 μL ; blue trace 5 μL , green trace 1 μL , light blue trace 0.5 μL and red trace 0.1 μL , using three different short chromatographic columns, (A) L = 10 mm FPP (1.7 μm , 2.1 \times 10 mm), (B) L = 10 mm SPP (2.7 μm , 2.1 \times 10 mm), and (C) L = 10 mm FPP (2.5 μm , 2.1 \times 10 mm). Generic conditions: flow rate 0.3 mL/min; gradient 30 to 45 % B in 0.8 min; temperature 80 $^{\circ}\text{C}$; UV detection 280 nm.

3. Results and discussion

3.1. Volumetric sample load

3.1.1. Impact of injection conditions in RPLC

To evaluate the effect of injection conditions in RPLC mode [16], several biopharmaceutical samples (intact mAb, reduced mAb and intact therapeutic protein) were analysed using columns with different geometries (variable length, different particle types and sizes). Fig. 1 illustrates the results obtained for the analysis of the reduced rituximab heavy chain (50 kDa) on three ultra-short 10 mm columns packed with 1.7 and 2.5 μm fully porous particles (FPP) and the column packed with 2.7 μm superficially porous particles (SPP). With these very short columns, the gradient time was obviously very short (only 0.8 min), which corresponds proportionally to a gradient time of 12 min on a 150 mm column. As expected, the performance obtained on the column packed with 2.5 μm FPP (Fig. 1C) were significantly lower than those obtained on the column of the same type (FPP), but packed with 1.7 μm particles (Fig. 1A), owing to the change in particle size and the direct relationship between the chromatographic efficiency and the inverse of the particle size [17]. On the other hand, the separation obtained with the column packed with 2.7 μm SPP (Fig. 1B) was quite comparable to that obtained with the 1.7 μm FPP column. This can be explained by the improvement in eddy dispersion and mass transfer resistance (A and C terms of a plate height equation), which is the dominant source of chromatographic peak dispersion when analysing macromolecules possessing very low diffusivity [18,19]. On the two most promising columns (FPP 1.7 μm and SPP 2.7 μm), it was possible to partially separate the main isoform as well as two hydrophobic variants eluted after the main peak. The separation of the last peak appears to be slightly better on the SPP 2.7 μm column, confirming the value of using columns packed with superficially

porous particles for protein analysis (Fig. 1B).

Focusing on the effect of the injected volume on the separation quality, five injections of the reduced antibody were performed on each column, with injection volumes ranging from 0.1 to 10 μL . It is important to note that the experimentally measured dead volumes for the three ultra-short columns used in this study were very low, ranging from 26 to 29 μL . Irrespective of the injected volume and the column used, the effect on the separation quality appears to be minimal, with peaks showing a moderate time shift (retention time was reduced by 2.1 - 4.5% when changing the injection volume from 0.1 and 10 μL on the three different ultra-short columns) and limited additional broadening (peak width increased by 29% on the maximum, when changing the injection volume from 0.1 and 10 μL on the three different ultra-short columns). To verify this observation, we calculated the peak widths at half height ($W_{1/2}$) obtained on the three ultra-short columns, as well as on the 50 and 150 mm reference columns, the latter two columns were packed with fully porous 1.7 μm particles. In these experiments the gradient times were systematically adjusted in direct proportion to the column length. Fig. 2 illustrates the normalization of peak widths ($w_{1/2}/t_0$) and injection volumes ($V_{\text{inj}}/V_{\text{col}}$), to have a fair comparison between columns having different lengths and gradient times. To construct Fig. 2, anakinra (a therapeutic protein of about 17 kDa) has been chosen as a model protein. Looking first at the raw data experimentally obtained ($W_{1/2}$ as a function of injected volume (V_{inj})) and plotted in Fig. 2A, significant differences in $W_{1/2}$ were observed depending on the column length, while the shapes of the curves remain comparable (increase in $W_{1/2}$ between an injection volume of 0 and 2 μL , followed by a more or less pronounced plateau depending on the column length, between 2 and 10 μL). The 150 mm column systematically produces wider peaks than the 50 mm column, which in turn produces wider peaks than the 10 mm columns, which all appear to be quite close. This behaviour, which

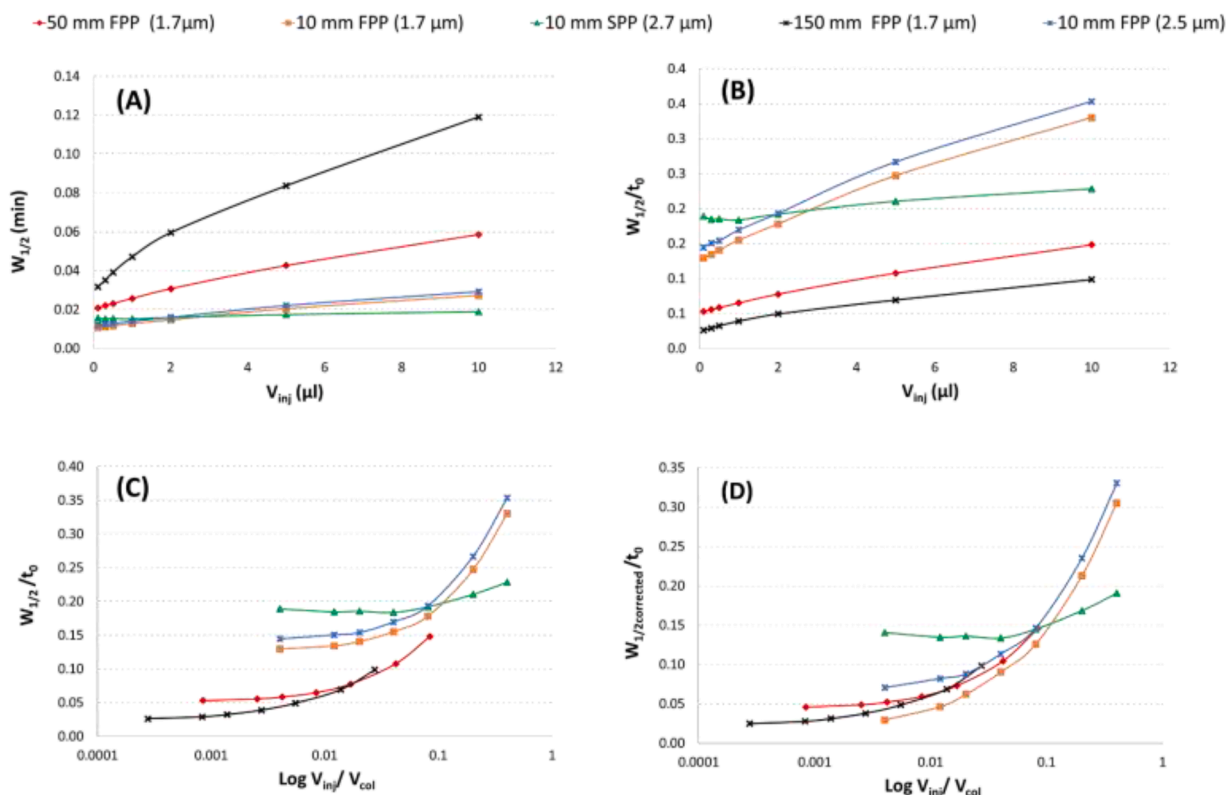


Fig. 2. Peak width plots obtained in RPLC when injecting 0.1, 0.3, 0.5, 1, 2, 5 and 10 μL of anakinra solution (0.5 mg/mL) for five different columns $d_p = 1.7, 2.5$ and 2.7 μm and lengths of 10, 50 and 150 mm. Columns: 1.7 μm , 2.1 \times 10mm, orange trace; 2.5 μm , 2.1 \times 10mm, blue trace; 2.7 μm , 2.1 \times 10mm, green trace; 1.7 μm , 2.1 \times 50 mm, red trace; and 1.7 μm , 2.1 \times 150 mm, black trace. Several plots are shown (A) absolute peak width ($W_{1/2}$) vs. volumetric loadability (μL), (B) relative peak width ($W_{1/2}/t_0$) vs. volumetric loadability (μL), (C) relative peak width ($W_{1/2}/t_0$) vs. relative volumetric loadability ($\text{Log } V_{\text{inj}}/V_0$), and (D) relative peak width corrected for the extra column contribution ($W_{1/2\text{corrected}}/t_0$) vs. relative volumetric loadability ($\text{Log } V_{\text{inj}}/V_0$).

is entirely logical, is related to the significantly longer gradient time on the longer columns and also to the fact that column peak variance is proportional to the square of the column volume. To focus solely on the effect of injection volume on peak width, without taking into account the variation in peak width due to the change in column length, the experimental width at half-height was divided by the experimentally measured dead time ($W_{1/2}/t_0$), to obtain a relative peak width value. The dead time was experimentally measured by injecting uracil, after subtracting the instrumental contributions measured in the absence of a column (extra-column volume and offset time) and the extra-bed contributions measured by extrapolation to a column length of zero [8]. These contributions are far from being negligible when working with ultra-short columns [3]. Fig. 2B shows the results obtained after data reprocessing. The ranking of the columns was now very different, the largest (50 and 150 mm long) columns resulted in the lowest relative peak width ($W_{1/2}/t_0$). The 10 mm columns appear to be quite similar, but notable differences were observed between the FPP and SPP columns. It appears that the short SPP column offers better performance, particularly for injection volumes greater than 2 μL , with the differences between SPP and FPP columns become more pronounced as the injected volume increases. Another aspect to consider for a reliable comparison of the effect of injection conditions on peak shape with columns of different sizes is the use of the ratio of injected volume to column dead volume (V_{inj}/V_{col}) on the graphical representation. Due to the very large differences in V_{inj}/V_{col} values that can be observed, a logarithmic scale was used. The corresponding data are reported in Fig. 2C. The results were similar to those shown in Fig. 2B, with a clear increase in relative peak widths with increasing relative injection volume, irrespective of column length. However, it is the two short FPP columns that were the most strongly affected by peak broadening at larger injection volumes.

Finally, the observed “apparent” peak width values were corrected for extra-column dispersion, by subtracting the extra-column variance from the observed total peak variance. This gives the intrinsic peak width related only to the column ($W_{1/2 \text{ corrected}}$) – free from system

dispersion. If the columns are identically packed and the impact of injection volume is the same, all the curves should be superimposed. As shown in Fig. 2D, all the FPP type columns behave in a fairly similar way, with almost overlapping curves that tend to remain fairly flat at low injection volumes (less than 1 μL), followed by a sharp rise for injection volumes between 1 and 10 μL , which for the FPP 1.7 μm , 2.1 \times 10 mm column corresponds to a relative injected volume value of 0.04 and 0.40, respectively. However, the relative peak broadening ($W_{1/2 \text{ corrected}}/t_0$) was always more pronounced for the short vs. long columns at the same injection volume. In addition, a notable difference was observed for the short SPP type column, which performed quite differently to the other 10 mm columns, with poorer performance at injection volumes of less than 2 μL and better performance at 5 or 10 μL injected.

In order to compare the effect of the injection conditions on the observed peak widths, the graph in Fig. 2C ($W_{1/2}/t_0$ vs. $\log V_{inj}/V_{col}$) was used for the rest of the study (such plots include system contributions, and is therefore more realistic to illustrate the experimentally attainable peak widths). Fig. 3 shows the results obtained for the five columns employed to analyze the three reference samples (i.e. intact mAb, reduced mAb and intact therapeutic protein). Here again, the injection volume ranged from 0.1 to 10 μL . Irrespective of the sample analysed, the short 10 mm SPP column (2.7 μm) always seemed to behave quite differently from the FPP columns. This behaviour was already highlighted in Fig. 2 and can be attributed to the very different morphology of the particles, leading to different kinetic performance and loading capacity. In addition, the SPP material is silica-based, while the FPP particles are hybrid-based materials. Many macromolecules are prone to form non-specific interactions with silica surfaces and thus may elute in broader peaks. One should also consider the differences in average pore diameter (450 \AA for SPP and 300 \AA for FPP) and pore size distribution too between the studied SPP and FPP particles. Nevertheless, the overall performance of 10 mm SPP column was never far from the two other 10 mm columns. If we focus on the 10, 50 and 150 mm FPP columns packed with 1.7 μm FPP particles (orange, red and black traces), the 10 mm

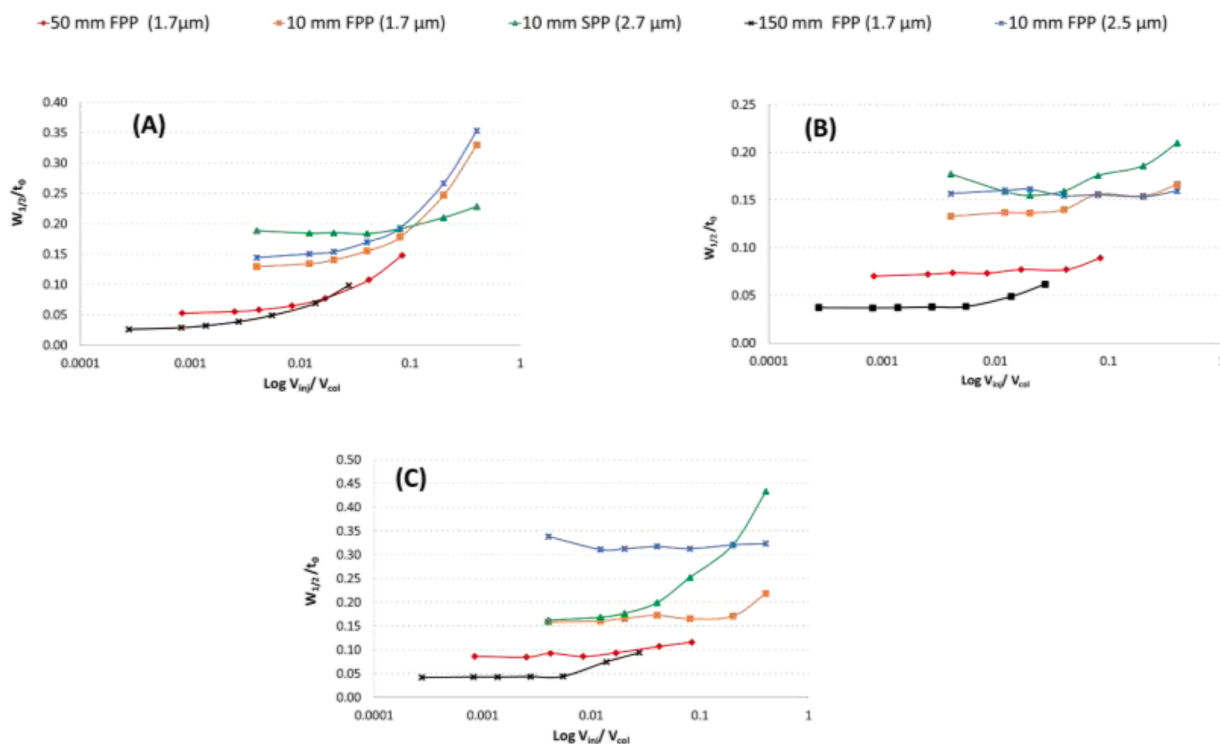


Fig. 3. Relative peak width vs. relative volumetric load plots obtained in RPLC when injecting 0.1, 0.3, 0.5, 1, 2, 5 and 10 μL of (A) anakinra (0.5 mg/mL) (B) reduced Rituximab (0.5 mg/mL) and (C) intact rituximab (0.5 mg/mL). Columns: 1.7 μm , 2.1 \times 10 mm, orange trace; 2.5 μm , 2.1 \times 10 mm, blue trace; 2.7 μm , 2.1 \times 10 mm, green trace; 1.7 μm , 2.1 \times 50 mm, red trace; and 1.7 μm , 2.1 \times 150 mm, black trace.

column systematically produces wider relative peaks than the 50 and 150 mm columns, regardless of the sample analysed. This behaviour can be attributed to the poorer packing quality of the ultra-short columns, as can be observed from the smallest injected volumes. In addition, it can be seen that the overloading effects (slope of the curve for the highest log V_{inj}/V_{col} values) appear to be more pronounced for the therapeutic protein anakinra (Fig. 3A) than for the reduced (Fig. 3B) or intact (Fig. 3C) monoclonal antibodies. For the reduced and intact mAb samples, which are larger than anakinra (50 and 150 kDa vs. 17 kDa), there is indeed virtually no effect of injected volume on peak widths at half height. This behaviour can possibly be linked to the on/off retention mechanism, which is more pronounced with larger molecules.

Based on these observations, it can be concluded that the injection volume is not a very critical parameter when using ultrashort columns for the analysis of therapeutic proteins in RPLC, except in special cases. There might be several reasons to explain this behaviour. First, it is important to remember that the protein samples were systematically diluted with pure water. As water is the weakest solvent in RPLC, a strong focusing effect of the injected band at the column inlet is expected, which limits significantly the physical width of the peak. Furthermore, as high molecular weight proteins undergo an on/off retention mechanism, the difference in eluent strength between the initial gradient conditions (70 % H₂O / 30 % ACN) and the sample diluent (100 % H₂O) is massive, which further enhances the phenomenon of band focusing at the column inlet. Finally, even with an injected sample volume corresponding to about 40% of the volume of the column used, its impact on the quality of the separation remains very limited. This observation suggests that it may be possible to inject large volumes on ultra-short columns to maximise sensitivity and thus improve detection limits, without too much impact on peak shapes, in particular

when analyzing intact or reduced mAb samples.

3.1.2. Impact of injection conditions in IEX

Next to RPLC mode, the effect of injection conditions was also assessed in ion exchange chromatography. The CEX mode is commonly used to characterise the charge variants of biopharmaceutical products. This mode is more widely used than anion exchange (AEX), due to the rather basic isoelectric points of most therapeutic proteins, especially mAbs. For analyses performed in CEX mode on very short columns, the detector was changed. Indeed, the UV detector used in this work produces a very strong tailing/broadening on the chromatographic peaks when a purely aqueous mobile phase is used. This phenomenon was attributed to the material used to build the UV detector cell (lightpipe technology), which is responsible for significant adsorption of proteins. For this part of the work, a fluorescence detector (FLD) was therefore used, incorporating a cell made of a different material that limits adsorption phenomena. The use of this FLD detector does not alter the conclusions regarding the effect of injection conditions on the chromatographic peaks.

Fig. 4 shows the chromatograms obtained on the 15 and 20 mm CEX columns (ultra-short columns) and the 50 mm CEX columns (reference column) having the same characteristics (chemistry, column internal diameter, particle diameter) when analysing an intact rituximab sample. Gradient times (6, 8 and 20 min) were adjusted according to the column length to maintain constant normalized gradient slopes. For each tested column, several chromatograms corresponding to injection volumes between 0.1 and 10 μ L were overlaid. Fig. 4 shows that the influence of the injection conditions on the quality of the separation was rather limited. In fact, when the injection volume was increased from 0.1 to 10 μ L, there was a slight change in the retention time (between 1 and 3.4%

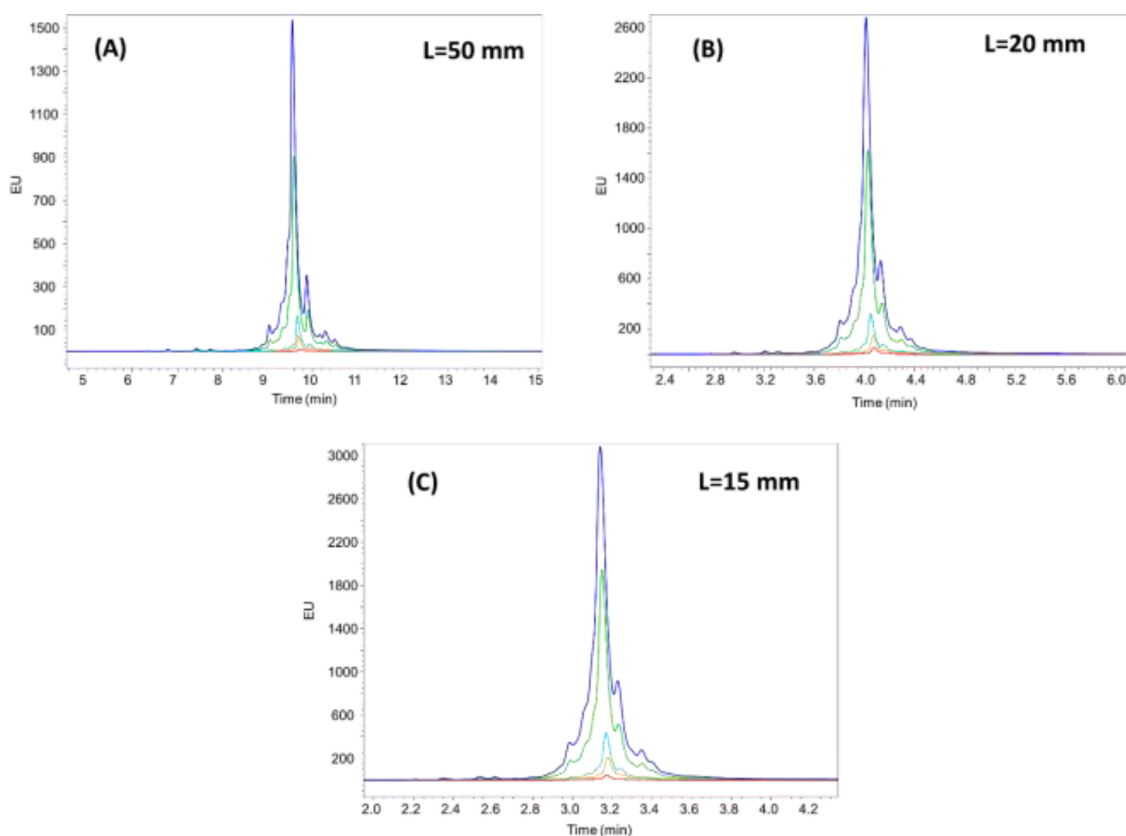


Fig. 4. Volumetric load in CEX mode. Charge variants separation of intact rituximab (0.5 mg/ml) by CEX using different column lengths (A) 3 μ m, 2.1 \times 50 mm; (B) 3 μ m, 2.1 \times 15 mm; (C) 3 μ m, 2.1 \times 15 mm. Chromatograms corresponding to different injected volumes, i.e. dark blue trace 10 μ L; green trace 5 μ L, light blue trace 1 μ L, orange trace 0.5 μ L and red trace 0.1 μ L. Generic conditions: flow rate 0.2 mL/min; gradient 30 to 50 % B in 6 min (L = 15 mm), 8 min (L = 20 mm) and 20 min (L = 50 mm); temperature 25°C; FLD detection with λ_{ex} = 280 nm, λ_{em} = 360 nm.

depending on the length of the selected column) and a very reasonable peak broadening (in the order of 30% maximum).

These initial observations were confirmed by the results shown in Fig. 5, showing the relative half-height peak widths ($W_{1/2}/t_0$) vs. relative injected volumes (V_{inj}/V_0) for the three columns used in this work (15, 20 and 50 mm) and 2 representative samples (anakinra and rituximab). Irrespective of the sample considered, the curves for the 15 and 20 mm columns were almost superimposed, whereas the relative half-height peak width values were found to be lower for the 50 mm column. This result can be explained by the fact that the columns used in ion exchange are packed with non-porous particles and therefore their dead volume is much lower than in RPLC mode for the same length, as already demonstrated elsewhere [4]. It is therefore expected that the shortest columns are more affected by the extra column volume and therefore produce significantly wider peaks than columns of conventional dimensions. Another factor to consider is the quality of the packing for columns of different lengths. Very short columns are prototypes whose packing conditions have not been fully optimised, unlike standard columns, and the loss in performance observed in Fig. 5 can also be attributed to this phenomenon. In any case, the shift observed in the curves between the short and the standard columns cannot be directly attributed to the injection conditions, as this behaviour was observed whatever the injection volumes, including the lowest one (0.1 μL). Fig. 5A and B also show that the shape of the curves remains strictly identical (U-shape) and that a slight loss of performance was observed at the largest injection volumes (5 and 10 μL). The U-shape curves were unexpected; the probable reason is the very low column volume due to the non-porous nature of the packing material and thus to the very small intrinsic peak variance. When injecting very small volumes, the column peak variance is expected to be very small and thus more affected by extra-column dispersion. Nevertheless, this increase in $W_{1/2}/t_0$ values remains quite reasonable and allows us to conclude that the influence of the injection conditions in CEX mode was very limited. This behaviour is directly related to the nature of the injection solvent, since the two samples (anakinra and rituximab) are formulated in an aqueous saline solution and then diluted very extensively with pure water (the final concentration of the samples was only 0.5 mg/ml). Given that the concentration of salts in the sample analysed was almost negligible and that pure water is the weakest eluent solvent in CEX mode (compared to an aqueous saline solution), we observe focusing effect at the column inlet and therefore a negligible impact of injection conditions. As proteins are also subject to an on/off retention mechanism in IEX, this focusing effect is even amplified. Finally, in CEX mode, it is possible to inject relatively large volumes into ultra-short columns, with a limited impact on the peak shapes.

3.1.3. Impact of injection conditions in HILIC

Finally, the effect of injection conditions was also assessed in HILIC mode. This mode is now increasingly used to characterise protein glycoforms at the intact or subunit level [20]. As prototype ultra-short

HILIC columns were not available at the time of the study, we initially focused on the shortest column commercially available, namely a 50 mm column length. Standard analytical conditions (60°C, 0.3 mL/min and gradient from 78 to 64 % ACN) were used, based on previous works from our laboratory [21,22]. Fig. 6 shows the chromatograms obtained with anakinra for various injection volumes and different concentrations (Fig. 6). These experiments were also performed with insulin (using 85-71% ACN gradient) and a reduced rituximab sample (using 72-64% ACN gradient). The experimental observations were similar regardless of the analysed sample, therefore only the results obtained with anakinra are presented here.

Fig. 6A clearly shows the effect of the injection conditions under HILIC conditions for injection volumes comprised between 0.5 and 2 μL . In the present case, the HILIC column has a dead volume of 107 μL , which means that the injected volume represents a maximum of 2% of the column dead volume. Such a value is very low compared to the experiments previously carried out in RPLC and CEX modes. Nevertheless, the effect of the injection is already significant, with either splitting of peak corresponding to anakinra or a partial breakthrough of the peak in two zones (a minor peak eluted at the expected retention time and a major peak eluted at the column dead time). These effects are clearly related to huge differences in elution strength between the sample diluent and the mobile phase. In this example, the sample was diluted in a 50/50 ACN/H₂O mixture as a compromise value to maintain acceptable protein solubility and limit differences in eluent strength between the diluent and mobile phase. However, the mobile phase was much weaker in terms of eluent strength than the sample diluent, as it contains a higher proportion of ACN. The sample diluent can therefore give rise to undesirable effects on the chromatographic separation, which may range from slight broadening to severe peak deformation or even breakthrough [23,24]. For an injection volume of 0.5 μL , the retained peak shows a wide range of deformations and three retained peaks appear instead of only one single peak corresponding to anakinra species. When the injection volume was increased (1 or 2 μL), the retention factor of the analyte at the head of the column at the time of injection was so low that some of the analyte passes through the column with very little interaction with the stationary phase and therefore elutes very close to the column dead time. This phenomenon is known as breakthrough, and generate a severe loss in sensitivity. Based on these observations, it is clear that an injection volume of 0.5 μL is already too high for a 50 \times 2.1 mm HILIC column. However, by further reducing the volume injected, the peak areas gradually decrease and cannot be detected anymore. In other words, it is clear that the injection conditions in HILIC mode are already very critical when analysing proteins on a 50 mm column and that it cannot be envisioned to use an even shorter column, unless an alternative solution is found to inject the protein sample in HILIC mode, as recently suggested by Taylor *et al.* for small molecules [25].

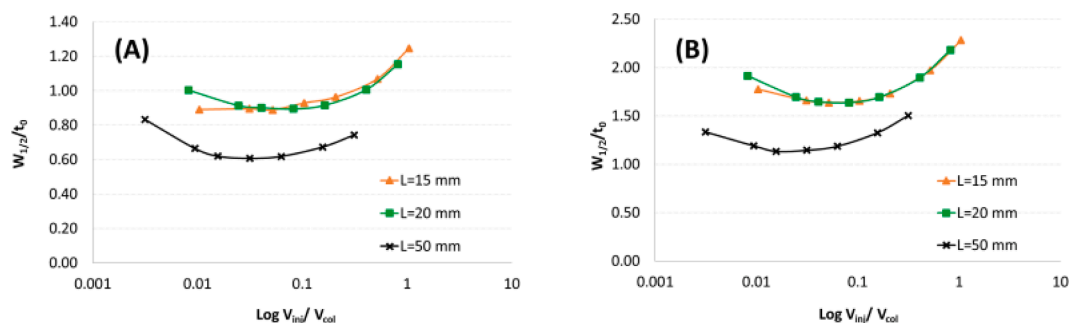


Fig. 5. Relative peak width vs. volumetric load plots obtained in CEX when injecting 0.1, 0.3, 0.5, 1, 2, 5 and 10 μL of (A) intact rituximab (0.5 mg/mL) and (B) anakinra (0.5 mg/mL). Columns: 3 μm , 2.1 \times 15 mm, orange trace; 3 μm , 2.1 \times 20 mm, green trace; and 3 μm , 2.1 \times 50 mm, black trace.

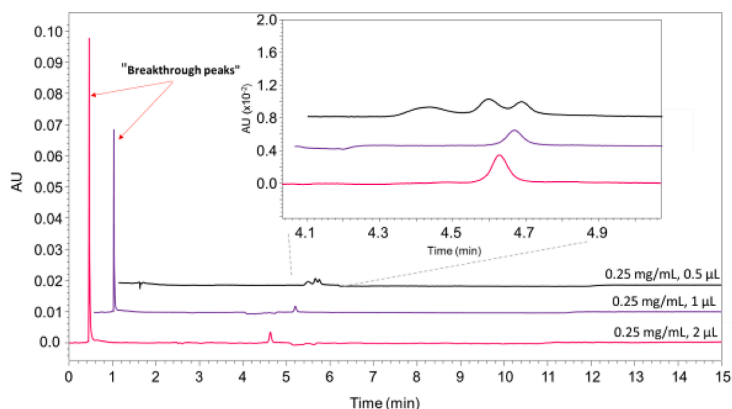


Fig. 6. HILIC chromatograms of anakinra sample. 0.5 μL (black trace), 1 μL (purple trace) and 2 μL (pink trace) of injection at 0.25 mg/mL. Generic conditions: flow rate 0.3 mL/min; gradient 78 to 64 % B in 10 min; column 300 \AA , 1.7 μm , 2.1 \times 50 mm; temperature 60 $^{\circ}\text{C}$; sample diluent 50/50 (ACN/water); and UV detection 280 nm.

3.2. Thermodynamic sample load

When the concentration of the injected sample increases (by maintaining the same injected volume), the equilibrium isotherm might be no longer linear, and thus impacts the ideal elution profile and broadens the peaks. Therefore, analysts used to inject samples at sufficiently low concentrations to avoid mass overload, and to obtain Gaussian, nearly symmetrical and sharp peaks. Here, we studied the effect of sample concentration on apparent peak width, when fixing the injected volume to a rather low value (1 μL), but loading different sample masses onto the very low volume ultra-short columns. Relative peak widths were then plotted as a function of relative mass load.

In RPLC, very similar behavior has been observed for all the different solutes. Fig. 7 shows a representative example (anakinra). The curves corresponding to different column lengths (column volume or mass) converge at high mass load, but they show significant differences in peak widths at very low mass loads. At low mass load (i.e. $m_{\text{inj}}/m_{\text{col}} \leq 0.05 - 0.06$), the longest column provides the thinnest peak, while the short columns provide apparently broader peaks. However, beyond a “cut-off” value of relative mass load ($m_{\text{inj}}/m_{\text{col}} \geq 0.05 - 0.06$), the loading curves run very close to each other, suggesting no (or negligible) difference in observed peak width at higher mass load. The reason for these significant differences at low mass load is probably due to the larger contribution of system dispersion to the intrinsic column dispersion (the latter is proportional to the square of column volume). Based on the obtained results, it is reasonable to say that if relatively large mass load is applied

(i.e. sample mass is larger than 5 - 6% of the stationary phase mass), then ultra-short columns will provide very similar apparent efficiency than conventional column formats. However, this apparent equivalence occurs only at the ascending part of the loading curves, suggesting entering into the non-linear range of the equilibrium isotherm.

In IEX, a different behavior was observed compared to RPLC. Different column lengths always resulted in different relative peak widths (no crossing point on the curves). The trends were very similar for each solute and figure 8 shows a representative example (anakinra). As one can see, the curves run horizontally up to $m_{\text{inj}}/m_{\text{col}} \approx 0.1$ (10% mass loaded), and then the slopes of the curves start to increase suddenly, suggesting that the non-linear range of the adsorption isotherms is reached. So, the mass loading capacity of IEX short columns is larger than the RPLC columns (the same observation was found for volumetric sample load). The curves obtained on the 15 and 20 mm long IEX columns run very close to each other, and they perform about 1.4 times relatively broader peaks compared to the 50 mm long column. Approximately the same rate of difference was observed between the 15 and 20 mm long columns compared to the 50 mm long one, when studying volumetric load. The reasons of the lower “apparent efficiency” for the ultra-short IEX columns here is probably the same as discussed in section 3.1.2., namely the relatively large extra-bed volume and poorer packing quality of the ultra-short columns, and also the relatively larger impact of system dispersion on observed peak widths (which is due to the non-porous nature of IEX packings, resulting in very low column volume and thus to very small intrinsic column peak variance). Please

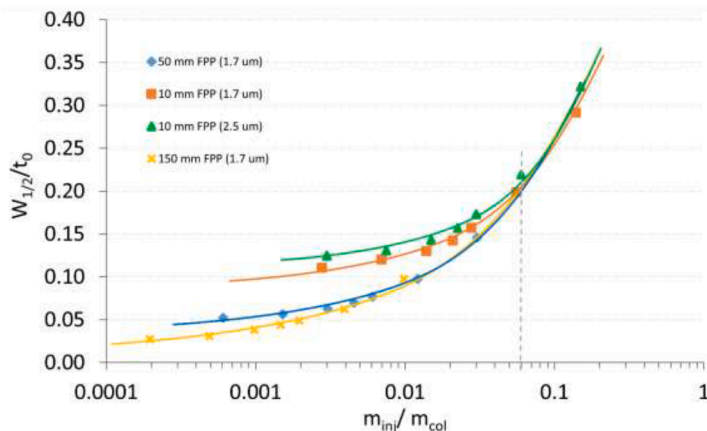


Fig. 7. Relative peak width as a function of relative sample mass loaded in RPLC when injecting various concentrations of anakinra sample at a fixed injection volume. Columns: 1.7 μm , 2.1 \times 10 mm (orange trace), 2.5 μm , 2.1 \times 10 mm (green trace), 1.7 μm , 2.1 \times 50 mm (blue trace) and 1.7 μm , 2.1 \times 150 mm (yellow trace).

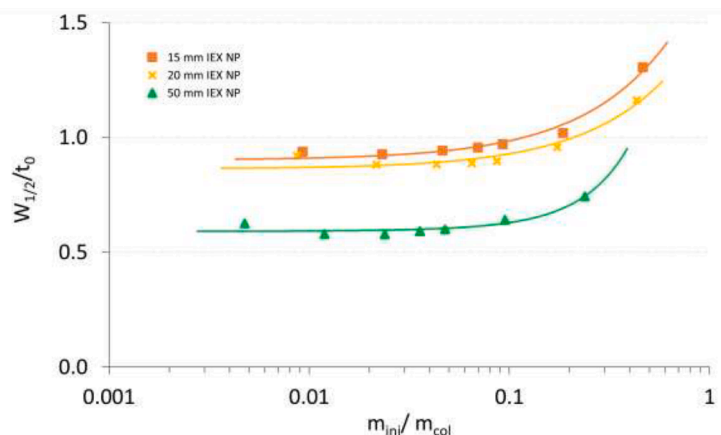


Fig. 8. Relative peak width as a function of relative sample mass loaded in IEX when injecting various concentrations of anakinra sample at a fixed injection volume. Columns: 3 μm , 2.1 \times 15 mm (orange trace), 3 μm , 2.1 \times 20 mm (yellow trace) and 3 μm , 2.1 \times 50 mm (green trace).

also note, that relative peak widths are always larger in IEX vs. RPLC. Indeed, the relative peak width ($w_{1/2}/t_0$) is comprised between 0.6 and 1.2 for IEX, while it ranges between 0.03 and 0.35 for RPLC.

4. Conclusions

As a rule of thumb, the applied injection volume should not exceed 10% of the effective column volume, and similarly, the injected sample mass should not exceed the 10% of the mass of the stationary phase, to avoid any detrimental effects related to volumetric or mass (thermodynamic) overload, respectively. Since volumetric overload is proportional to column volume, one might have the impression that ultra-short columns ($L < 50$ mm) may suffer from band broadening and/or peak distortion due to overload even when very low sample volume is injected.

In this study, the effect of injected sample volume on apparent efficiency (peak width) has been systematically studied in gradient elution mode for various chromatographic modes (i.e. RPLC, IEX and HILIC). Since the main application area of ultra-short columns is the analysis of macromolecules (following on-off elution mechanism), small to large proteins have been studied.

It is important to emphasize that macromolecules are exclusively analyzed in gradient elution mode, which is a consequence of their on-off behavior. In RPLC and IEX modes, water (in absence of salts or at very low ionic strength) is the weakest solvent that can be used. Therefore, when introducing the sample to the column using water as diluent, its inlet retention is inherently very high, so the sample band will be physically focused at the head of the column, and its spatial variance will be very limited. In these conditions, most of the sources of pre-column dispersion are therefore compensated. Then, once the solute starts migrating, the solute band will benefit from a very strong gradient band compression (again due to their on-off like elution behavior). Therefore, in the end, it is logical to conclude that injection volume in RPLC and IEX has little impact on band broadening. Indeed, we found that in RPLC, the impact of injected volume was low, $V_{inj} \leq 0.1 V_{col}$ has no detrimental effect on the separation quality. Its effect was even lower in IEX, where as high as $V_{inj} \leq 0.4 V_{col}$ sample injection still resulted in appropriate peak shape and separation quality.

However, in HILIC, since the sample diluent is stronger than the initial mobile phase strength, peak splitting (partial breakthrough) or total breakthrough can be easily observed already at very low injected volumes (i.e. $V_{inj}/V_{col} \leq 0.01$). This means that $V_{inj} \leq 0.1 - 0.2 \mu\text{L}$ should be applied for 10 \times 2.1 and 20 \times 2.1 mm columns, respectively, which is the limit of current LC instrumentations.

To conclude, for RPLC and IEX separations, ultra-short columns can be applied on current instrumentations without overloading the column,

while ultra-short HILIC columns are more difficult to use from the volumetric load point of view since they require very low injected volumes.

When studying mass load (which in practice is less relevant, since sample manipulation – dilution – is not preferred for the analysis of biopharmaceutical products), similar behavior was found. Indeed, the largest relative mass can be injected onto IEX columns without detrimental effects on separation (up to 10% sample to sorbent mass).

CRediT authorship contribution statement

Raquel Perez-Robles: Investigation, experimental work, visualization, Writing; **Szabolcs Fekete:** Conceptualization, Writing - reviewing and Editing; **Natalia Navas:** Funding acquisition, Writing - review & editing; **Davy Guillarme:** Conceptualization, Writing - reviewing and Editing

Declaration of Competing Interest

The authors declare the following financial interests/personal relationships which may be considered as potential competing interests: ACQUITY, UPLC, Empower and BEH are trademarks of Waters Technologies Corporation. MabThera is a trademark of F. Hoffmann-La Roche AG. Kineret is a trademark of Swedish Orphan Biovitrum AB.

Data availability

Data will be made available on request.

Acknowledgements

Raquel Pérez-Robles currently holds a postdoctoral position granted by the Junta de Andalucía, Spain (ref:DOC_01694).

References

- [1] M.R. Nejadnik, T.W. Randolph, D.B. Volkin, C. Schöneich, J.F. Carpenter, D.J. A. Crommelin, W. Jiskoot, Postproduction Handling and Administration of Protein Pharmaceuticals and Potential Instability Issues, *J. Pharm. Sci.* 107 (2018) 2013–2019, <https://doi.org/10.1016/j.xphs.2018.04.005>.
- [2] S. Fekete, B. Bobály, J.M. Nguyen, A. Beck, J.L. Veuthey, K. Wyndham, M. A. Lauber, D. Guillarme, Use of ultrashort columns for therapeutic protein separations. Part 1: Theoretical considerations and proof of concept, *Anal. Chem.* 93 (2021) 1277–1284, <https://doi.org/10.1021/acs.analchem.0c04082>.
- [3] A. Murisier, V. D'Atri, S. Pirner, V. Larraillet, S. Fekete, M. Lauber, D. Guillarme, Ultra-Fast Middle-Up Reversed Phase Liquid Chromatography Analysis of Complex Bispecific Antibodies Obtained in Less Than One Minute, *Pharmaceutics* 14 (2022), <https://doi.org/10.3390/pharmaceutics14112315>.

- [4] J.A. Navarro-Huerta, A. Murisier, J.M. Nguyen, M.A. Lauber, A. Beck, D. Guillarme, S. Fekete, Ultra-short ion-exchange columns for fast charge variants analysis of therapeutic proteins, *J. Chromatogr. A*. 1657 (2021), 462568, <https://doi.org/10.1016/j.chroma.2021.462568>.
- [5] B. Duivelshof, A. Zöldhegyi, D. Guillarme, M. Lauber, S. Fekete, Expediting the chromatographic analysis of COVID-19 antibody therapeutics with ultra-short columns, retention modeling and automated method development, *J. Pharm. Biomed. Anal.* 221 (2022), <https://doi.org/10.1016/j.jpba.2022.115039>.
- [6] Z. Guo, J. Pang, Z. Liu, On the journey exploring nanoscale packing materials for ultra-efficient liquid chromatographic separation, *J. Chromatogr. Open*. 2 (2022), 100033, <https://doi.org/10.1016/J.JCOA.2022.100033>.
- [7] K. Mejía-Carmona, J. Soares da Silva Burato, J.V.B. Borsatto, A.L. de Toffoli, F. M. Lanças, Miniaturization of liquid chromatography coupled to mass spectrometry: 1. Current trends on miniaturized LC columns, *TrAC Trends Anal. Chem.* 122 (2020), 115735, <https://doi.org/10.1016/J.TRAC.2019.115735>.
- [8] S. Fekete, I. Kohler, S. Rudaz, D. Guillarme, Importance of instrumentation for fast liquid chromatography in pharmaceutical analysis, *J. Pharm. Biomed. Anal.* 87 (2014) 105–119, <https://doi.org/10.1016/J.JPBA.2013.03.012>.
- [9] F. Gritti, C.A. Sanchez, T. Farkas, G. Guiochon, Achieving the full performance of highly efficient columns by optimizing conventional benchmark high-performance liquid chromatography instruments, *J. Chromatogr. A*. 1217 (2010) 3000–3012, <https://doi.org/10.1016/J.CHROMA.2010.02.044>.
- [10] N. Wu, A.C. Bradley, C.J. Welch, L. Zhang, Effect of extra-column volume on practical chromatographic parameters of sub-2- μ m particle-packed columns in ultra-high pressure liquid chromatography, *J. Sep. Sci.* 35 (2012) 2018–2025, <https://doi.org/10.1002/jssc.201200074>.
- [11] G. Desmet, K. Broeckhoven, Extra-column band broadening effects in contemporary liquid chromatography: Causes and solutions, *TrAC Trends Anal. Chem.* 119 (2019), 115619, <https://doi.org/10.1016/J.TRAC.2019.115619>.
- [12] F. Gritti, G. Guiochon, Overload behavior and apparent efficiencies in chromatography, *J. Chromatogr. A*. 1254 (2012) 30–42, <https://doi.org/10.1016/J.CHROMA.2012.07.015>.
- [13] T. Werres, T.C. Schmidt, T. Teutenberg, The influence of injection volume on efficiency of microbore liquid chromatography columns for gradient and isocratic elution, *J. Chromatogr. A*. 1641 (2021), <https://doi.org/10.1016/j.chroma.2021.461965>.
- [14] A.C. Sanchez, J.A. Anspach, T. Farkas, Performance optimizing injection sequence for minimizing injection band broadening contributions in high efficiency liquid chromatographic separations, *J. Chromatogr. A*. 1228 (2012) 338–348, <https://doi.org/10.1016/J.CHROMA.2012.01.038>.
- [15] J. Dai, P.W. Carr, D.V. McCalley, A new approach to the determination of column overload characteristics in reversed-phase liquid chromatography, *J. Chromatogr. A*. 1216 (2009) 2474–2482, <https://doi.org/10.1016/J.CHROMA.2009.01.036>.
- [16] V. D'Atri, A. Murisier, S. Fekete, J.L. Veuthey, D. Guillarme, Current and future trends in reversed-phase liquid chromatography-mass spectrometry of therapeutic proteins, *TrAC Trends Anal. Chem.* 130 (2020), 115962, <https://doi.org/10.1016/J.TRAC.2020.115962>.
- [17] D.V. McCalley, Some practical comparisons of the efficiency and overloading behaviour of sub-2 μ m porous and sub-3 μ m shell particles in reversed-phase liquid chromatography, *J. Chromatogr. A*. 1218 (2011) 2887–2897, <https://doi.org/10.1016/j.chroma.2011.02.068>.
- [18] R. Hayes, A. Ahmed, T. Edge, H. Zhang, Core-shell particles: Preparation, fundamentals and applications in high performance liquid chromatography, *J. Chromatogr. A*. 1357 (2014) 36–52, <https://doi.org/10.1016/J.CHROMA.2014.05.010>.
- [19] S. Fekete, E. Oláh, J. Fekete, Fast liquid chromatography: The domination of core-shell and very fine particles, *J. Chromatogr. A*. 1228 (2012) 57–71, <https://doi.org/10.1016/J.CHROMA.2011.09.050>.
- [20] A. Periat, S. Fekete, A. Cusumano, J.L. Veuthey, A. Beck, M. Lauber, D. Guillarme, Potential of hydrophilic interaction chromatography for the analytical characterization of protein biopharmaceuticals, *J. Chromatogr. A*. 1448 (2016) 81–92, <https://doi.org/10.1016/J.CHROMA.2016.04.056>.
- [21] V. D'Atri, A. Goyon, B. Bobaly, A. Beck, S. Fekete, D. Guillarme, Protocols for the analytical characterization of therapeutic monoclonal antibodies. III – Denaturing chromatographic techniques hyphenated to mass spectrometry, *J. Chromatogr. B*. 1096 (2018) 95–106, <https://doi.org/10.1016/J.JCHROMB.2018.08.013>.
- [22] B. Bobály, V. D'Atri, A. Beck, D. Guillarme, S. Fekete, Analysis of recombinant monoclonal antibodies in hydrophilic interaction chromatography: A generic method development approach, *J. Pharm. Biomed. Anal.* 145 (2017) 24–32, <https://doi.org/10.1016/J.JPBA.2017.06.016>.
- [23] S. CHAPEL, F. Rouvière, V. Peppermans, G. Desmet, S. Heinisch, A comprehensive study on the phenomenon of total breakthrough in liquid chromatography, *J. Chromatogr. A*. 1653 (2021), 462399, <https://doi.org/10.1016/J.CHROMA.2021.462399>.
- [24] J. Ruta, S. Rudaz, D.V. McCalley, J.L. Veuthey, D. Guillarme, A systematic investigation of the effect of sample diluent on peak shape in hydrophilic interaction liquid chromatography, *J. Chromatogr. A*. 1217 (2010) 8230–8240, <https://doi.org/10.1016/J.CHROMA.2010.10.106>.
- [25] M.R. Taylor, J. Kawakami, D.V. McCalley, Managing sample introduction problems in hydrophilic interaction liquid chromatography, *J. Chromatogr. A*. 1700 (2023), 464006, <https://doi.org/10.1016/J.CHROMA.2023.464006>.